Journal of Inflammation Research

Dovepress
Taylor & Francis Group

Open Access Full Text Article

ORIGINAL RESEARCH

Electroacupuncture Attenuates Colitis in Mice Through Activation of Vagus Cholinergic Antiinflammatory Pathways

Zhengyang Qu, Min Luo, Xiaoyu Liu, Yangshuai Su, Xianghong Jing

Meridian Research Center, Institute of Acupuncture and Moxibustion, China Academy of Chinese Medical Sciences, Beijing, People's Republic of China

Correspondence: Yangshuai Su; Xianghong Jing, Email suyangshuai@163.com; jxhtjb@263.net

Background: Colitis impairs life quality, and treatments are limited. Acupuncture may engage vagal anti-inflammatory pathways, but the precise circuits are unclear.

Objective: This study aimed to examine the effects of electroacupuncture (EA) at "Shangjuxu" (ST37) on murine colitis and the involvement of the cholinergic vagus system.

Methods: Mice were divided into control, model, EA (electro-acupuncture), and MLA (EA with α7nAChR antagonist) groups. A colitis model was induced in mice by freely drinking a 2.5% dextran sodium sulfate (DSS) solution for 7 days. Colitis severity was assessed via body weight, colon length, and H&E staining. Proximal colon cytokines were measured by MSD assay. Immunofluorescence evaluated activation of ChAT-positive neurons in the dorsal motor nucleus of the vagus (DMV) and local colon cholinergic markers. Anatomical interactions between ChAT-positive fibers and α7nAChR-positive cells were observed. Vagal efferent fiber activity was recorded electrophysiologically.

Results: EA at ST37 significantly reduced body weight loss and proximal colon tissue damage in colitis mice ($P < 0.05$). These beneficial effects were blocked by the α7nAChR antagonist MLA. Levels of five pro-inflammatory cytokines (TNF-α, IL-6, CXCL1, IL-1β, IL-5) were elevated in the model group but decreased following EA treatment ($P < 0.05$). Colitis increased activation of ChAT-positive neurons in the DMV, and EA further enhanced this activation ($P < 0.05$). The reduced α7nAChR content in the proximal colon of model mice was restored to near-normal levels by EA ($P < 0.05$). EA also significantly increased the activation of cervical vagal efferent fibers ($P < 0.05$). Anatomical associations between ChAT-positive fibers and α7nAChR-positive cells were observed in the EA group.

Conclusion: EA at ST37 alleviates inflammation in colitis mice likely by activating ChAT-positive neurons in the DMV. This stimulates vagal efferent nerves, modulates α7nAChR-positive cells in the proximal colon, and engages the vagal cholinergic anti-inflammatory pathway.

Keywords: electroacupuncture, vagus nerve, ulcerative colitis, neuroimmune regulation, cholinergic anti-inflammatory

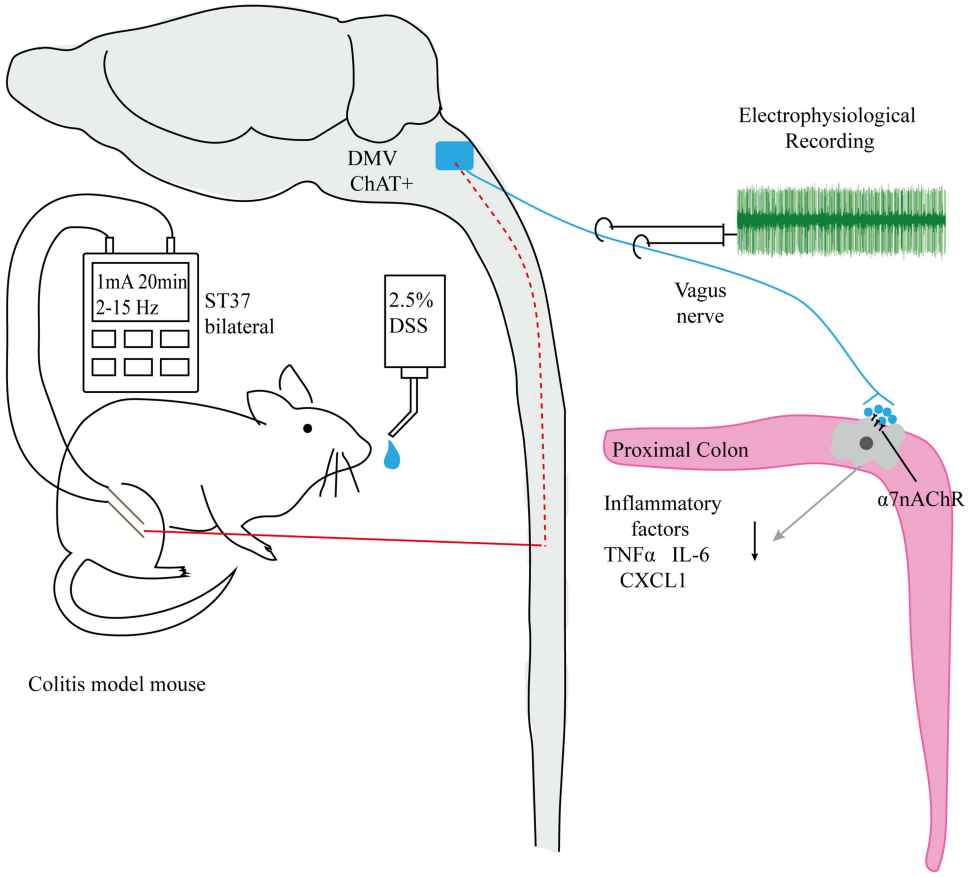
Introduction

Colitis is a chronic inflammatory disease. It can affect the entire colon, including the ascending, transverse, descending, and sigmoid colon.[1–3] This condition predominantly occurs in young and middle-aged individuals between 30 and 40 years old. It significantly impacts their work capacity and overall quality of life.[1–3] The pathological mechanism involves a complex interplay between multiple immune organs and neuroimmune reflexes.[4–6] Currently, the main clinical treatments for colitis include corticosteroids, pro-inflammatory cytokine antagonists, and surgery.[7,8] However, these approaches face considerable challenges. Exogenous hormones cause significant side effects, and single-target drugs often have limited efficacy.[7,8] While these medications may temporarily relieve symptoms, they cannot prevent disease recurrence and are accompanied by various side effects.[1,8] Therefore, both patients and clinicians urgently need to explore novel treatment strategies for colitis.

https://doi.org/10.2147/JIR.S582737
Received: 27 November 2025
Accepted: 5 March 2026
Published: 11 March 2026

© 2026 Qu et al. This work is published and licensed by Dove Medical Press Limited. The full terms of this license are available at https://www.dovepress.com/terms.php and incorporate the Creative Commons Attribution – Non Commercial (unported, v4.0) License (http://creativecommons.org/licenses/by-nc/4.0/). By accessing the work you hereby accept the Terms. Non-commercial uses of the work are permitted without any further permission from Dove Medical Press Limited, provided the work is properly attributed. For permission for commercial use of this work, please see paragraphs 4.2 and 5 of our Terms (https://www.dovepress.com/terms.php).

Graphical Abstract



The parasympathetic cholinergic neuroimmune pathway is a critical immune neuromodulation network in mammals. It represents a fundamental mechanism for modulating inflammatory responses and maintaining internal homeostasis.[9] Choline acetyltransferase-positive (ChAT+) neurons in the dorsal motor nucleus of the vagus (DMV) send excitatory signals. These signals travel through vagal efferent fibers. The fibers innervate and coordinate multiple thoracic and abdominal organs. This helps alleviate visceral inflammatory infections by activating specific immune effectors.[9] The vagus nerve innervates colonic segments, including the ascending and transverse colon.[10,11] Research suggests that acetylcholine binding to α7 nicotinic acetylcholine receptors (α7nAChR) on colon macrophages can mitigate colitis. This effect is achieved by reducing the local release of pro-inflammatory factors.[12,13] Building on this, researchers have explored electrical stimulation of the cervical vagus nerve. This method harnesses similar cholinergic mechanisms to alleviate colitis.[14–18] It indicates that activating the vagal pathway holds promise for ameliorating colonic inflammation. Clinical studies inspired by the cholinergic anti-inflammatory pathway show that appropriate cervical vagus nerve stimulation can suppress inflammation. This effect primarily depends on exciting vagal efferent fibers.[19,20] However, this intervention initially requires complex cervical surgery. It poses certain safety risks and trauma to patients. In contrast, electroacupuncture (EA) stimulation can activate the parasympathetic system. It may represent a safer and more convenient intervention. EA is capable of eliciting physiological excitation and modulation of vagus nerve activity.

Over the past decade, research on acupuncture's regulation of the autonomic nervous system has explored various physiological and pathological mechanisms. Clinical efficacy trials have also been conducted.[5] Among these diverse research avenues, the study of its "anti-inflammatory effect" has become the most prominent topic. Particular emphasis is placed on the cholinergic anti-inflammatory mechanism.[5] Notably, the majority of highly cited references in this field

focus on inflammation. Gastrointestinal and cardiovascular diseases are the most actively investigated conditions within this context.[5] The remote regulatory effects of acupuncture can be precisely mediated through distinct somatosensory-autonomic reflex pathways. This provides a refined understanding of its mechanisms of action.[21–24] several studies have reported on the mechanisms of electroacupuncture (EA) in alleviating ulcerative colitis (UC). A series of foundational studies have demonstrated that EA can improve colonic tissue damage scores and disease activity indices in colitis model animals. It also repairs damaged tight junctions between mucosal epithelial cells and reduces the expression of inflammatory factors such as TNF-α and IL-6.[25,26] However, existing basic research primarily focuses on observing the effects of EA. The mechanistic analysis is often limited to single, localized immune-related cellular or molecular events within the colon.[27]

Extensive basic and clinical evidence indicates that acupuncture can effectively improve colitis. However, the specific neuroimmune pathways through which acupuncture exerts its anti-inflammatory effects remain unclear. This knowledge gap significantly hinders the refinement of the theoretical framework for acupuncture's anti-inflammatory action and its broader clinical translation. Our team's preliminary research suggests that electroacupuncture can significantly activate ChAT-positive neurons in the DMV of rats.[28] This finding provides the hypothesis for the present study: Electroacupuncture at ST37 may alleviate colonic inflammation by activating the cholinergic vagal neuroimmune pathway. This study aims to systematically investigate the mechanism by which electroacupuncture at ST37 alleviates inflammation in the proximal colon of mice with colitis. The investigation will be conducted from the perspective of the vagal cholinergic neuroimmune pathway. This pathway involves the dorsal motor nucleus of the vagus (DMV), vagal efferent fibers, and α7nAChR-positive cells in the proximal colon.

Materials and Methods

Animals

All experimental mice were obtained from commercial suppliers at 4 weeks of age. They were housed in a specific pathogen-free (SPF) facility under controlled conditions (12-hour light/dark cycle, 24 ± 2°C) with free access to standard chow. After a 4-week adaptive feeding period, experiments began when mice reached 8 weeks of age. The study included male C57BL/6J mice (20–22 g) from Sperphar Biotechnology, as well as Ai14 and ChAT-Cre homozygous mice from South Model Organisms Center. Offspring of ChAT-Cre × Ai14 crosses (ChAT-Ai14 mice) were also used. A total of 40 C57BL/6 mice were randomly divided into four groups (n=10 per group): normal control (C), model (M), electro-acupuncture (EA), and EA with methyllycaconitine citrate (MLA). An additional 12 mice were assigned to C and EA groups (n=6 each) for vagal electrophysiology. Five ChAT-Ai14 mice were used for immunofluorescence staining. Mice were group-housed (5–6 per cage). All animal procedures followed the NIH Guidelines for the Care and Use of Laboratory Animals and the ARRIVE guidelines.

Colitis Model Induction

Colitis was induced in mice from the M, EA, and MLA groups by administering 2.5% dextran sodium sulfate (DSS) in drinking water for 7 days.[29] Control group mice received plain drinking water for the same duration.

Anesthesia

Throughout the study, anesthesia was performed using 1.5% isoflurane mixed with air. Mice were first placed in a gas induction chamber (ventilation rate: 0.4 L/min). After full anesthesia, a nose cone adapter was used to maintain anesthesia (ventilation rate adjusted to 0.1 L/min). During procedures, mice were kept on a 38°C heating pad. Vital signs (heart rate, respiration, limb/mucous membrane color) were monitored continuously. Vaseline eye ointment was applied to prevent corneal injury.

Sample Collection and Processing

If euthanasia was required for tissue collection, anesthetized mice were placed in a sealed chamber with carbon dioxide to induce asphyxia. For inflammatory and molecular analyses, proximal colon samples were collected from 7 mice per

group to measure local cytokines and α7nAChR content. A small segment of proximal colon from each mouse was also taken for hematoxylin and eosin (HE) staining. For neuroanatomical studies, 3 mice per group underwent transcardiac perfusion with 4% paraformaldehyde; their brainstems were collected for immunofluorescence staining of the dorsal motor nucleus of the vagus (DMV). In the vagal electrophysiology cohort, neural recordings were obtained from the additional 12 mice. For the ChAT-Ai14 mice, proximal colon segments were processed to visualize anatomical interactions between ChAT-positive nerve fibers and α7nAChR-positive cells via immunofluorescence. All animals and their corresponding data were included in the final statistical analysis.

Intervention

Throughout the course of the experiment, on days 1, 3, 5, 7, and 9 of DSS administration, mice in the EA group underwent meticulous EA treatment at the ST37 while under anesthesia. The anatomical location of ST37 is on the posterior lateral side of the knee joint in mice, approximately 4 mm below the fibular head. Precision stainless steel acupuncture needles, measuring 0.18 mm in diameter and 13 mm in length, were delicately inserted into the bilateral ST37 regions to a precise depth of 3 mm. These needles were then seamlessly connected to electroacupuncture instrument, delivering tailored electrical stimulation at 1mA intensity, with a pulse width of 500 us, and an intermittent wave with a frequency range of 2–15Hz for an optimal duration of 20 minutes. During this intervention, meticulous attention was paid to ensure that the ST37 acupoint regions exhibited a harmonious muscle twitching in unison with the EA apparatus' frequency parameters, achieving the cherished state of "Deqi", signifying the effective activation of the acupuncture points. The electroacupuncture procedure for mice in the MLA group was the same as that for the EA group. However, 30 minutes before each electroacupuncture session, mice in the MLA group received an intraperitoneal injection of Methyllycaconitine citrate at a dose of 4.8 mg/kg. Mice in the C and M groups were anesthetized under similar conditions but did not receive the EA treatment. Before each intervention procedure, mice in the C, M, and EA groups were intraperitoneally injected with the same dose of saline as the MLA group, to eliminate confounding factors.

The Disease Activity Index (DAI)

DAI was employed to evaluate the mice from each experimental group, focusing on their fecal consistency and the presence of occult blood in their stool. The DAI, derived as the average of the Fecal Occult Blood Score and the Fecal Consistency Score, provides a comprehensive assessment of disease severity. The fecal consistency was graded on a scale ranging from 0 (hard feces) to 4 (very watery feces), with intermediate stages designated as semi-loose (1 point), loose (2 points), and watery (3 points). To determine the Fecal Occult Blood Score, a minute amount of feces was sampled and subjected to a colorimetric reaction using specific FOB reagents (color developer A followed by color developer B). The scoring criteria, based on the observed color change within a minute of reagent application, ranged from 0 (no color change) to 4 (obvious blood visible in feces), with intermediate stages indicated by faint purple-red coloration (1 point) and distinct purple-blue coloration within 10 seconds (2 points), or visible traces of blood (3 points). This DAI process was systematically executed on day 1 prior to modeling as a baseline measurement and subsequently, on a daily basis throughout the modeling period, spanning from day 1 to day 9, ensuring a comprehensive tracking of disease progression and treatment efficacy.[30]

Molecular Biology and Morphology Experiments

2.7.1 Detection of inflammatory cytokines/acetylcholine and acetylcholinesterase content in mouse colonic tissue using electro/photochemical luminescence ELISA technology:

Adhering to the instructions outlined in the MSD Multi-Factor Detection Kit, the provided 96-well plate was sealed and washed. Subsequently, 50μL of diluted mouse serum or colon tissue homogenate protein samples were added to each well. The plate was then incubated at room temperature on a shaking bed set at 750 rpm for a duration of 2 hours. After this incubation period, the plate underwent three wash cycles and was then supplemented with antibodies specific to the target inflammatory factors (encompassing CXCL1, IL-5, IL-12p70, IL-2, IL-4, IL-1β, TNF-α, IL-6, IL-10, and IFN-γ, amounting to a total of 10 factors, V-PLEX Proinflammatory Panel1 (mouse) Kit (K15048D G-series), MSD, inc., USA). The plate was incubated again under the same conditions for an additional 2 hours. Following three more wash cycles,

read buffer was added, and the levels of inflammatory cytokines were ultimately determined using the MSD Multi-Factor Detection Instrument, employing the electrochemiluminescence method for detection.

Immunofluorescence Experiment

Experimental mice were perfused with 4% paraformaldehyde via cardiac puncture, and the tissues were subsequently collected and stored in a −80°C freezer. Prior to the experiment, the required tissues were retrieved from the −80°C freezer and equilibrated in a cryostat set at −27°C for 30 minutes before undergoing frozen embedding and sectioning. After appropriate trimming, the tissues were flattened and securely fixed onto a specimen holder. An adequate amount of embedding agent was applied to fully envelop the tissues, which were then placed in the cryostat for low-temperature solidification. Once the embedding agent had completely solidified, sections were cut with a predetermined thickness of 20μm and carefully mounted onto glass slides. The sections were then rinsed three times with 0.1M PBS (PH=7.4), each rinse lasting 5 minutes, followed by incubation with PBST buffer at room temperature for 0.5 hours. This was succeeded by incubation in a solution consisting of 3% BSA and 10% goat serum (PBST) at room temperature for 1 hour. Subsequently, the sections were incubated with the primary antibody overnight on a shaker maintained at 4°C. On the following day, the sections were rinsed three times with PBS buffer, each rinse lasting 5 minutes, after which the secondary antibody was added and the sections were incubated at room temperature for 2 hours. They were then rinsed again three times with PBS buffer, each rinse lasting 10 minutes. The tissue sections were mounted onto glass slides using the floating section method, sealed with anti-fluorescence quenching mounting medium, and allowed to rest in the dark for 0.5 hours before being photographed. Observations and image acquisition were conducted using a confocal fluorescence microscope. One to three non-overlapping fields of view were selected, and the number of positive neurons as well as the brightness of positive fluorescence were quantified using ImageJ. (ab181023/ab302667/ab150105/ab150079 was used in this experiment, Abcam plc, UK).

Real-Time Quantitative Fluorescent PCR Experiment Procedure

Upstream primer for α7nAChR: CAGTGAGTGGAAGTTTGCG, downstream primer for α7nAChR: TTTGGGGCTGACATGAGGA. Upstream primer for ACTIN: CCATCTACGAGGGCTATGCT, downstream primer for ACTIN: CTTTGATGTCACGCACGATT. The Real-Time Quantitative Fluorescent PCR Experiment Procedure involves extracting Total RNA from samples using TRNzol reagent according to product instructions. Subsequently, RNA quality is assessed by measuring concentration and purity through ultraviolet absorption spectrometry, checking the A260/A280 ratio (which should be between 1.8–2.1), and calculating the concentration. Denaturing Agarose Gel Electrophoresis is then conducted, which entails preparing a gel with agarose, ultrapure water, 10×MOPS electrophoresis buffer, and formaldehyde solution. Samples (minimum 25ul) are loaded, the gel is placed in an electrophoresis tank, and 1×MOPS buffer is injected. Electrophoresis is performed, and the results are observed under ultraviolet transmission light. Following this, Reverse Transcription is carried out to synthesize cDNA using HiScript III 1st Strand cDNA Synthesis Kit (+gDNA wiper, R312-01, Nanjing Vazyme Biotech Co., Ltd., China), adhering to product instructions. This involves performing Genomic DNA Removal Reaction and Reverse Transcription Reaction, with incubation at specific temperatures. The cDNA is then stored in a −20°C freezer. For RealTime PCR Sample Detection, the Realtime PCR reaction system is prepared for all cDNA samples, which are loaded into a 96-well PCR plate. The PCR reaction is performed with specific temperature settings, and relative quantitative results are analyzed using the 2^-(ΔΔct) calculation formula, correcting for differences in cDNA content using internal reference protein mRNA.

Hematoxylin and Eosin (H&E) Staining Protocol for Mouse Proximal Colon Tissue

Proximal colon tissue samples were collected and immediately fixed in 4% paraformaldehyde for 24 hours at 4°C. The fixed tissues were then dehydrated through a graded series of ethanol solutions (70%, 80%, 90%, 95%, and 100%). This was followed by clearing in xylene and embedding in paraffin wax. Sections were cut at a thickness of 5 μm using a microtome and mounted on glass slides. For staining, the paraffin sections were first deparaffinized in xylene and rehydrated through a descending ethanol series to distilled water. The nuclei were stained with Harris hematoxylin solution for 5–8 minutes. After rinsing in tap water, the sections were differentiated in 1% acid alcohol for a few seconds. They were then blued in Scott's tap water substitute. Cytoplasm was counterstained with eosin Y solution for

1–3 minutes. Following staining, the sections were dehydrated through an ascending ethanol series, cleared in xylene, and finally mounted with neutral balsam under a coverslip. Stained slides were examined under a light microscope to assess general histoarchitecture, inflammatory cell infiltration, and tissue damage.

Surgical Exposure of the Cervical Vagus Nerve and Electrophysiological Recording Method

Surgical Exposure of the Cervical Vagus Nerve

After preparing the ventral neck skin of the mouse, make an incision approximately 1.5cm long along the midline of the ventral neck skin. Use forceps to bluntly separate the subcutaneous tissue and muscles, locating the left cervical vagus nerve attached between the trachea and the left carotid artery. Carefully isolate the nerve from surrounding tissues using a glass needle. Fill the space between the vagus nerve and the overlying muscle and tracheal tissues with sealing film, and apply warm paraffin oil at 37°C to isolate the vagus nerve from surrounding tissues while maintaining neural activity. Proceed to carefully dissect the nerve epineurium, then use a glass needle to divide the vagus nerve into fine bundles as much as possible. Subsequently, dissect the perineurium of these fine nerve bundles and ligate the vagus nerve near the thoracic end to eliminate any potential interference from afferent vagus nerve signals.

Electrophysiological Recording

For electrophysiological recording of the left cervical vagus nerve, utilize a platinum wire hook electrode to securely hook the nerve. Connect the electrode to an electrophysiological recorder, and after amplification by an AM1800 amplifier (AM System, USA), filter the signal (30Hz-20kHz) using a CED1401 data acquisition system and extract the discharge signal. Employ Spike2 v8.06 software for data display and storage. The electrophysiological recording is divided into the following distinct phases: a 30-minute post-surgery recovery period, a 10-minute baseline period, a 10-minute electroacupuncture intervention (or combined electroacupuncture intervention and brain nucleus illumination) period, and a final 20-minute post-intervention period.

Statistical Analysis

Statistical analysis was conducted using the SPSS V.12.0 (SPSS Inc., Chicago, Illinois, USA). Changes in body weight were analyzed using repeated measures ANOVA. For all other data, tests for homogeneity of variance and normal distribution were conducted first. For data meeting the assumptions of homogeneity of variance and normal distribution: for baseline data comparison, the Dunnett test was utilized; To analyze differences between groups, we employed a 1-way analysis of variance followed by the Student-Newman-Keuls post hoc test, or alternatively, a 2-way analysis of variance followed by the Bonferroni post hoc test; When analyzing variance differences between groups, the LSD method was selected for data analysis. In cases where the data did not adhere to a normal distribution or exhibit homogeneity of variance, the non-parametric Tamhane's T2 test was applied for analysis. A P value of less than 0.05 was considered statistically significant. The final data were presented in the format of mean ± SEM.

Results

Electroacupuncture at ST37 Significantly Ameliorates Weight Loss, DAI Scores, and Local Tissue Damage Throughout the Colon in a Mouse Model of Colitis

First, we elucidated the effects of electroacupuncture at ST37 intervention on the general physical condition and local colonic pathology of mice with colitis. According to our experimental data, normal mice exhibited a continuous increase in body weight over the next 9 days, reaching 107.18% on the 9th day. In contrast, mice in the M group, which drank 2.5% DSS solution, maintained a similar weight gain to normal mice for the first 5 days (105.48%). However, starting from the 6th day, the body weight of mice in the M group dropped rapidly (102.20%), falling below the initial weight by the 8th day and reaching 93.94% of the initial weight on the 9th day. Mice in EA groups showed similar weight curves to the M group for the first 7 days (101.97%). However, on the 8th and 9th days for the EA group (97.78%), the trend of weight loss slowed compared to the M group. The body weight of mice in the MLA group exhibited significant

fluctuations: it decreased sharply from Day 1 to Day 5 (91.57%), but then rebounded slightly over the next 2 days (95.15–99.14%), however during the last 2 days when DSS drinking was stopped, the body weight continued to decline (88.25%) (Figure 1A).

In terms of behavioral manifestations (DAI scores), differences were also observed among the 3 groups of mice drinking 2.5% DSS solution. During the first 7 days, the progressively worsening hematochezia and loose stools were similar across the C and M groups, peaking on the 7th day. Subsequently, on the 8th and 9th days, there was a certain degree of improvement in the loose stools and hematochezia C and M groups. Regarding the MLA group, from Day 3 until the animals were sacrificed, the degree of bloody stools and loose stools in this group of mice increased abnormally (Figure 1B). It is noteworthy that the EA group exhibited slightly better conditions regarding hematochezia and loose stools on the 7th, 8th, and 9th days compared to the M group. Regarding local colonic pathological damage, compared to normal mouse colonic tissue, the M and MLA group showed the most severe tissue structure damage and inflammatory

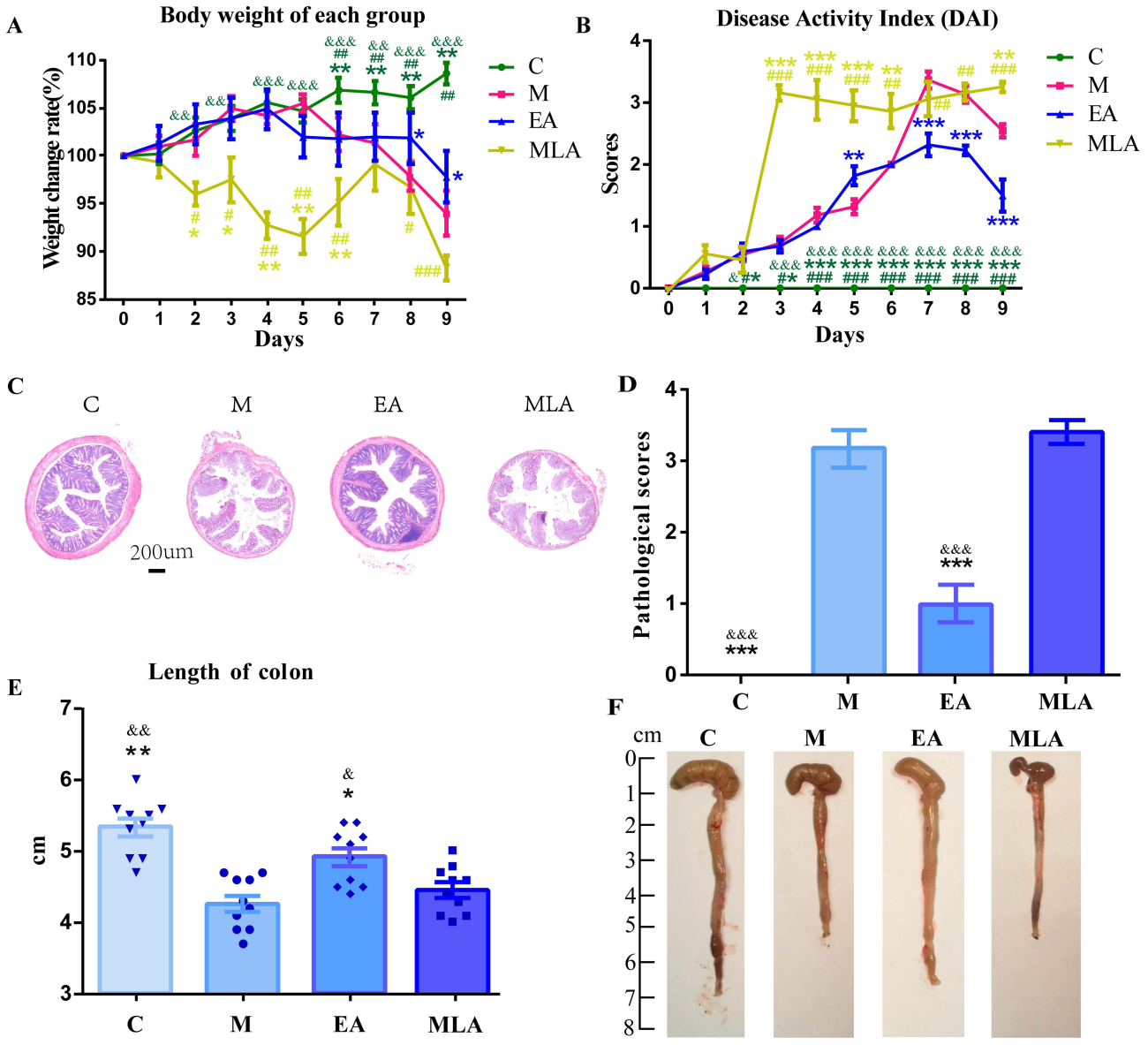


Figure 1 Representative results of colitic signs and local pathological changes in the proximal colon among different groups of mice. (**A**) Body weight change curve; (**B**) DAI score; (**C**) Representative histopathological images of the proximal colon; (**D**) Histopathological score; (**E**) Statistical analysis of colon length; (**F**) Example images of colon length and morphology in mice from each group. (**C**) control group; M: model group; EA: electroacupuncture group; MLA: electroacupuncture with methyllycaconitine citrate. Compared with the M group: * $P < 0.05$, ** $P < 0.01$, *** $P < 0.001$ vs M group; Compared with the EA group: $^{\#}$ $P < 0.05$, $^{\#\#}$ $P < 0.01$, $^{\#\#\#}$ $P < 0.001$; Compared with the MLA group: $^{\&}$ $P < 0.05$, $^{\&\&}$ $P < 0.01$, $^{\&\&\&}$ $P < 0.001$. n=10.

https://doi.org/10.2147/JIR.S582737

infiltration. While the EA group showed relatively mild damage and less inflammatory cell infiltration (Figure 1C and D). On the 9th day, after the mice were euthanized, we measured the length of the entire colon in each group. Given the previous results, it was unsurprising that the M or MLA group had a significantly shorter colon length compared to the other groups. Although the colon lengths of the EA were also shortened compared to normal mice, the differences were not statistically significant (Figure 1E and F).

Electroacupuncture at ST37 Partially Regulates Local Inflammatory Factors in Proximal Colitis

Having established the beneficial effects of ST37 electroacupuncture on the behavior, physical signs, and pathological scores of mice with proximal colitis, we delved deeper into exploring the alterations in local inflammatory cytokines within the proximal colonic tissue. Among the 10 inflammatory factors we examined in the colon of our colitis mouse model, In the local inflammatory factors of the proximal colon in the colitis mouse model we examined, six inflammatory factors including IFN-γ, TNF-α, IL-6, CXCL1, IL-1β, and IL-5 showed an increase in the M group compared to the C group, while they decreased in the electroacupuncture group. In our results, IL-2, IL-4, IL-10, and IL-12p70 did not appear to be involved in the progression of proximal colitis in mice (Figure 2).

Electroacupuncture at ST37 Activates ChAT-Positive Neurons in the DMV and Stimulates the Intestinal Cholinergic Anti-Inflammatory System

Although we have known that electroacupuncture at ST37 can improve the physical signs and behaviors of mice with colitis by regulating some local intestinal inflammatory factors, the underlying mechanisms of this effect remain unclear. Next, we preliminarily explored the activating effect of electroacupuncture at ST37 on the parasympathetic cholinergic anti-inflammatory system. Our immunofluorescence results showed that, compared with the control group (C), there was a significant increase in the activation of ChAT-positive neurons in the DMV region of the model group (M). Surprisingly, the activation of ChAT-positive neurons in the DMV region induced by electroacupuncture at ST37 was even greater than that in the M group (Figure 3).

Electroacupuncture at ST37 Activates the Vagus Nerve

Upon comprehensive analysis of the above results, the function of the vagus nerve, which connects the dorsal motor nucleus of the vagus (DMV) brain region to the local cholinergic anti-inflammatory system in the colon, becomes particularly significant. By examining the electrophysiological characteristics of the vagus nerve under ST37 electroacupuncture conditions, the anti-inflammatory effect of electroacupuncture can be effectively assessed. As illustrated, the discharge frequency of the vagus nerve in mice with colitis is significantly higher compared to the control group. (Figure 4A) Consistent with our DMV immunofluorescence results, electroacupuncture stimulation led to an increase in the discharge frequency of the vagus nerve. (Figure 4B) The surgical image of the electrophysiological recording of the efferent fibers of the mouse cervical vagus nerve is shown in Figure 4C.

There is an Anatomical Connection Between Cholinergic Nerve Fibers and α7 Receptor-Positive Immune Cells in the Proximal Colon

Next, we will observe the activation of the cholinergic anti-inflammatory system in the colon. We used ChAT-Ai14 tool mice to create a model and observed clear anatomical connections between ChAT positive nerve fibers and α7 receptor positive cells in the proximal colon after a single application of ST37-electroacupuncture(Figure 5A and B). Then we detected the local α7nAChR in the proximal colon of mice in each group. The α7nAChR content in the model group was significantly lower than that in the control group. The α7nAChR content in the electroacupuncture group increased compared to the model group and was close to that in the control group (Figure 5C).

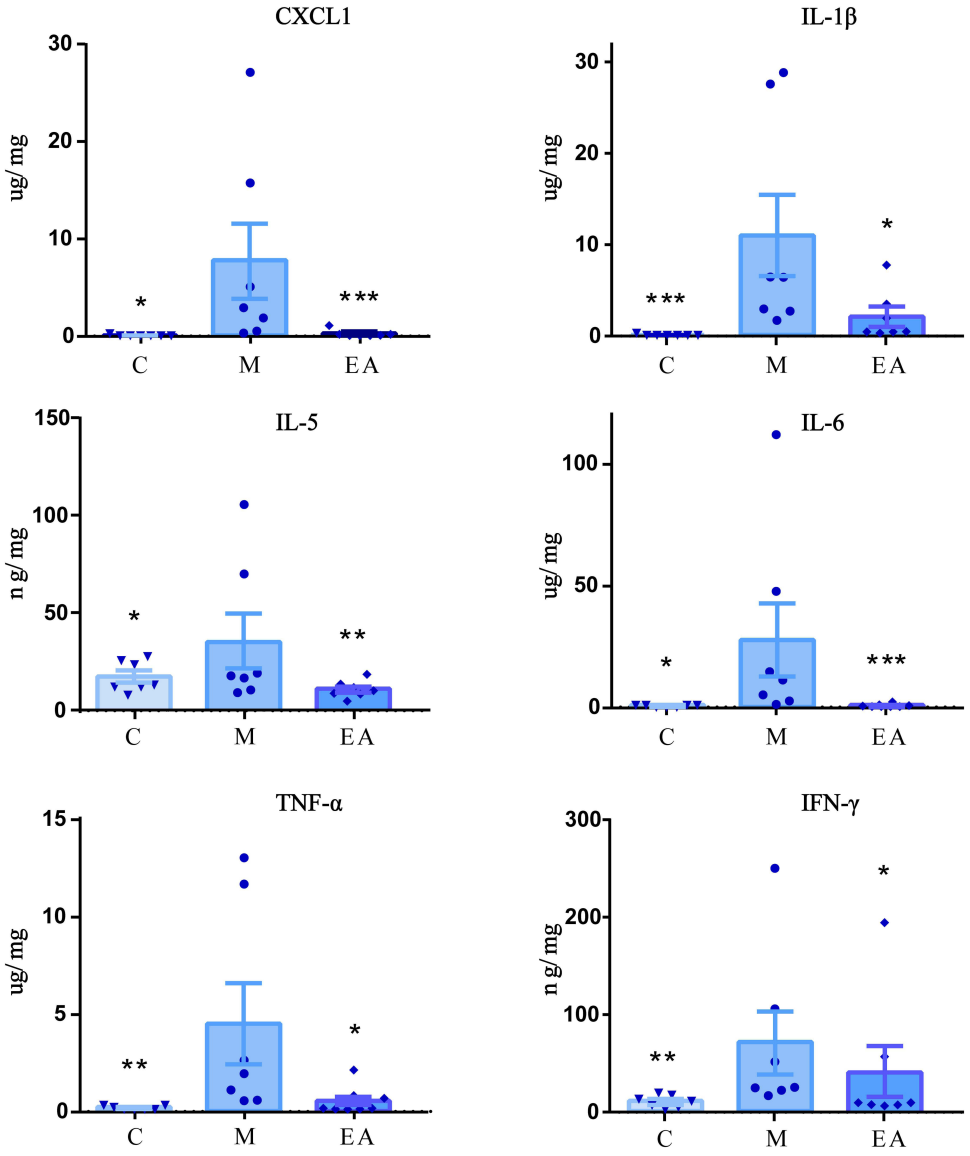


Figure 2 Expression levels of inflammatory cytokines with statistically significant differences (TNF-α, IL-6, CXCL1, IL-1β, IL-5, and IFN-γ) in the proximal colon of mice from each group. C: control group; M: model group; EA: electroacupuncture group. Compared with the M group: * $P < 0.05$, ** $P < 0.01$, *** $P < 0.001$. n=7.

Discussion

This study is based on the hypothesis that electroacupuncture at ST37 alleviates proximal colitis by activating the brainstem DMV-vagus nerve-colonic α7nAChR cholinergic anti-inflammatory pathway. Using a mouse model of colitis, we first confirmed the therapeutic effect of electroacupuncture at ST37. This was demonstrated by improvements in animal behavior, physical signs, and proximal colon pathology. We then analyzed changes in proximal colonic inflammatory cytokines across different groups to explore the mechanism of action. Furthermore, we observed that electroacupuncture at ST37 activated ChAT-positive neurons in the DMV and modulated the expression of α7nAChR-positive cells in the colon. An anatomical connection was confirmed between ChAT-positive nerve fibers and α7nAChR-positive cells. Finally, by recording activity in cervical vagal efferent fibers before, during, and after electroacupuncture, we linked the anti-colitis effects to the activation of specific central and peripheral neural pathways.

Fundamental research since the early 21st century has clarified the anatomical and functional links between the autonomic and immune systems. These autonomic-immune interactions are crucial in many pathological and physiological processes.[31] The autonomic nervous system, including its sympathetic and parasympathetic branches, regulates

https://doi.org/10.2147/JIR.S582737

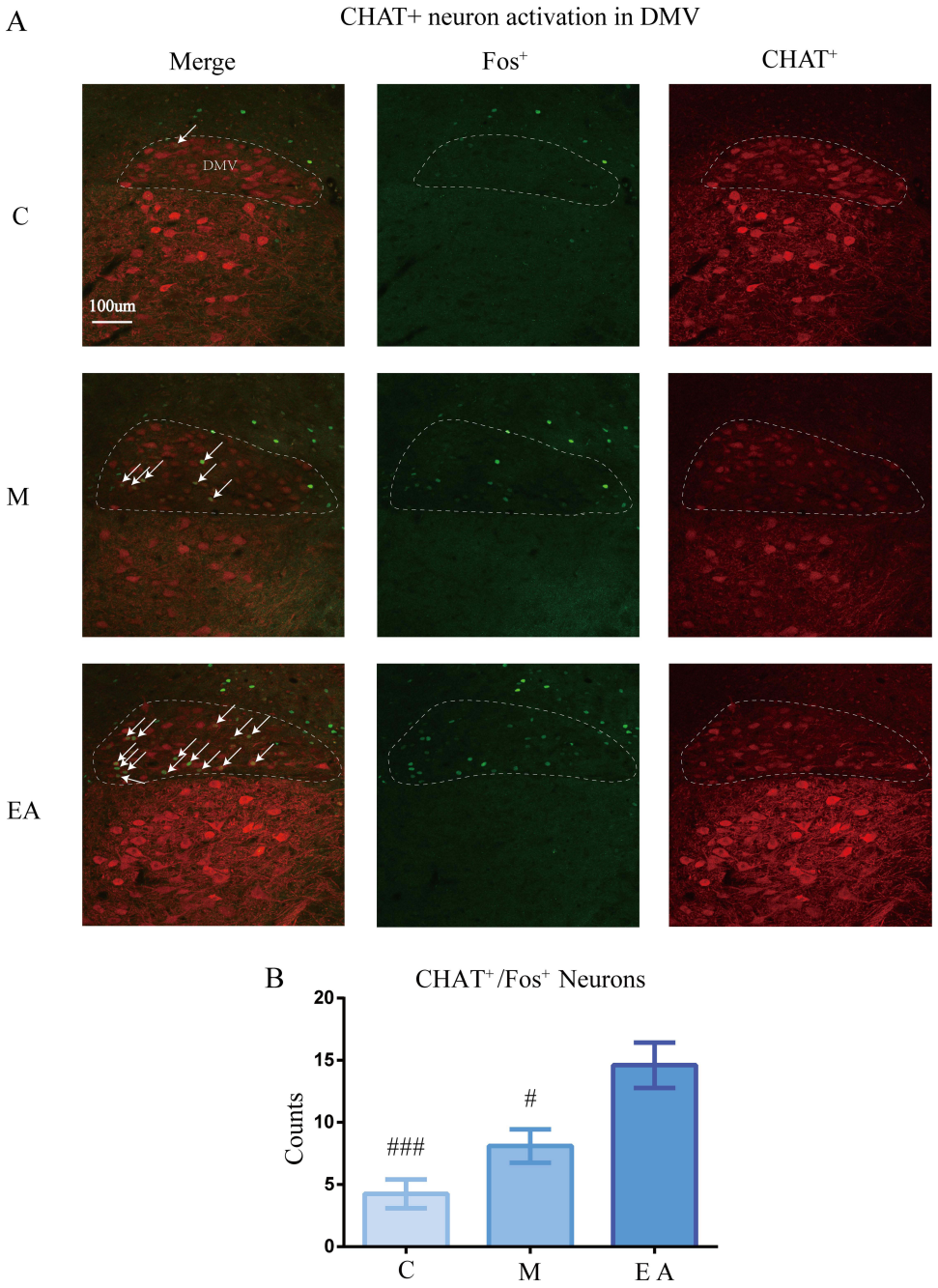


Figure 3 Co-expression of c-Fos in ChAT-positive neurons in the DMV nucleus across experimental groups. Green fluorescence indicates Fos expression, red fluorescence represents ChAT immunoreactivity, and double-labeled neurons are indicated by white arrows. (**A**) Statistical chart of the number of co labeled ChAT positive and Fos positive neurons in the DMV nucleus (**B**). C: control group; M: model group. Compared with the EA group: $^{\#}$ $P < 0.05$, $^{\#\#\#}$ $P < 0.001$. n=3.
Abbreviation: EA, Electroacupuncture group.

immune function from the skin to internal organs like the gut. This field is now a key focus in life science. Targeted activation of autonomic nerves to modulate organ immunity represents a promising new clinical approach.[32,33] In colitis, abnormal immune responses occur throughout the colon, involving complex interactions between immune organs and neuro-immune reflexes.[6] For example, DSS-induced colitis reduces neuronal activity in sympathetic ganglia like the coeliac-superior mesenteric ganglia.[34] Vagus nerve signaling reduces pro-inflammatory cytokine secretion (eg, IL-1β) by activating the α7nAChR on macrophages,[13,17] showing the parasympathetic pathway's beneficial role in reducing colon inflammation.[13,17,18,35,36] Chemogenetic activation of the parasympathetic nerve also decreases MPO activity and

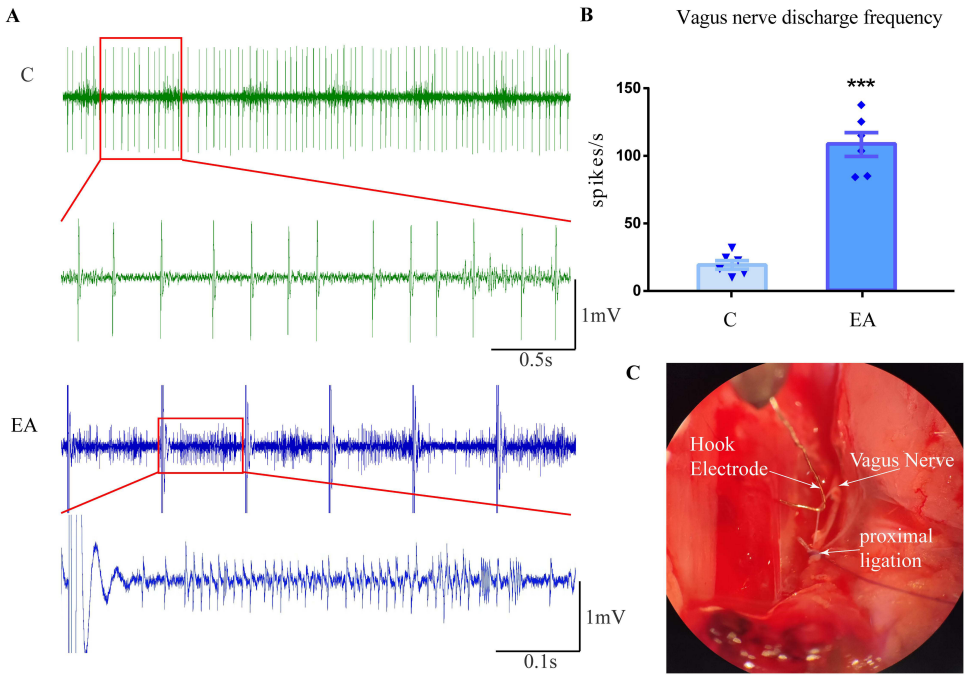


Figure 4 Changing in vagal efferent nerve excitability across experimental groups and the mechanism by which electroacupuncture at ST37 activates the cholinergic vagal pathway to ameliorate proximal colitis. (**A**) Representative traces of cervical vagus nerve discharge in control and model group mice, as well as during 2 Hz electroacupuncture at ST37. (**B**) Bar graph summarizing the discharge frequency in each group. (**C**) Surgical schematic diagram of electrophysiological recording using a hooked electrode attached to the thin bundle of the vagus nerve. Compared with the C group: ***P < 0.001. n=6.
Abbreviations: C, control group; EA, electroacupuncture group.

increases IL-10 in rat colitis models.[9] The role of the sympathetic nervous system in colitis is context-dependent. Pharmacological studies show the α2-receptor antagonist yohimbine reduces colonic MPO activity in DSS-mice, while the β-receptor agonist isoproterenol worsens damage.[37] Chemical sympathectomy with 6-OHDA significantly reduced local inflammation in model rats,[38] suggesting sympathetic excitation may disrupt colonic inflammatory balance. However, findings can be paradoxical. In TNBS-induced colitis, catecholamine levels in affected gut segments were lower than in controls.[39] Furthermore, models of sympathetic inhibition (eg, chemical denervation) have been shown to worsen DSS-induced colitis,[40,41] indicating an anti-inflammatory effect of sympathetic activation under those specific conditions.

Electrical stimulation of the cervical vagus nerve can activate cholinergic mechanisms to alleviate colitis.[17,18] This confirms the positive role of vagal pathway activation in improving colonic inflammation. Research by Borovikova et al demonstrated that direct vagus nerve stimulation triggers the cholinergic anti-inflammatory pathway.[42] This leads to acetylcholine release from efferent vagal fibers, which suppresses local immune cell activation and reduces pro-inflammatory cytokine release. Clinical studies indicate that cervical vagus nerve stimulation can suppress inflammation, primarily through efferent vagal fiber excitation.[19,20] However, this procedure requires invasive cervical surgery, posing safety risks and trauma. Stimulating the deeper sacral parasympathetic nerves is even more challenging. Additionally, implanted stimulators have non-rechargeable batteries, complicating long-term treatment. Whether direct nerve stimulation adequately mimics physiological function also requires further verification. In contrast, activating the parasympathetic system via peripheral stimulation may be a safer and more convenient intervention.

The findings of this study demonstrate that electroacupuncture applied at the acupoint ST37 (Shangjuxu) effectively activates efferent fibers within the cervical segment of the vagus nerve. This observed neural activation aligns with and substantiates previous reports in the literature regarding the ability of peripheral somatic stimulation to engage central autonomic pathways. Importantly, the physiological consequence of this vagal activation is a significant visceral anti-inflammatory effect. The magnitude of this anti-inflammatory action is comparable to the therapeutic outcomes achieved by direct electrical stimulation of the cervical vagus nerve itself, a more invasive procedural intervention. This parallel

https://doi.org/10.2147/JIR.S582737

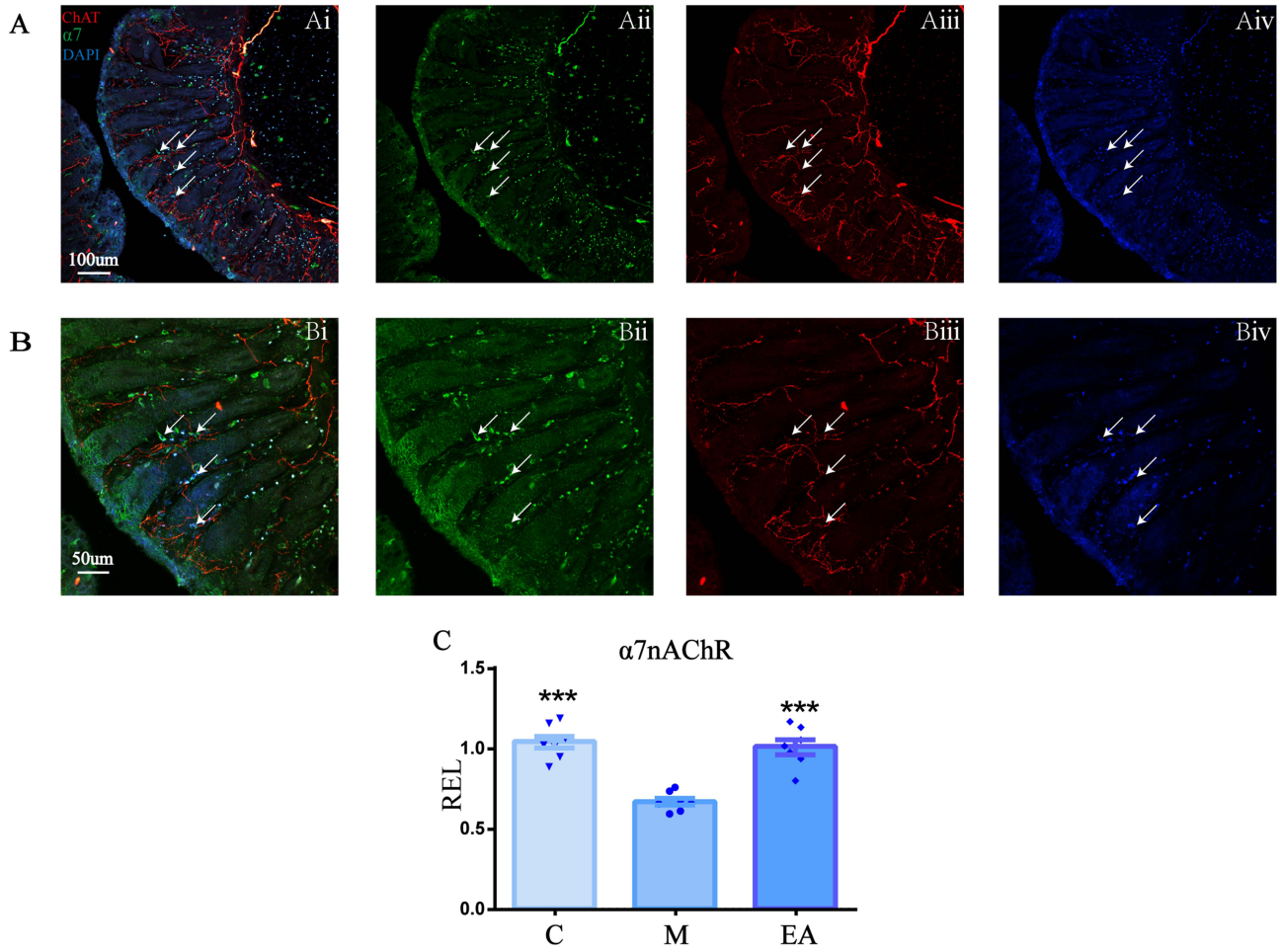


Figure 5 Anatomical connectivity and functional expression of the cholinergic system in the proximal colon following local electroacupuncture in mice. (**A** and **B**) Co-localization of ChAT-positive fibers and α7nAChR in the proximal colon of ChAT-Ai14 mice after electroacupuncture. (**C**) Expression levels of α7 nAChR in the proximal colon across experimental groups. C: control group; M: model group. Compared with the M group: *** $P < 0.001$. n=7.
Abbreviation: EA, Electroacupuncture group.

suggests that electroacupuncture can serve as a potent peripheral stimulus to harness the body's endogenous cholinergic anti-inflammatory system. By providing this mechanistic link, the study offers a concrete neuroanatomical and functional basis for the clinical benefits of acupuncture in treating inflammatory conditions like colitis. It underscores the potential of non-invasive, acupoint-based strategies to modulate systemic inflammation through well-defined neural circuits.

Beyond activating the vagal cholinergic system, electroacupuncture also crucially regulates local immune cells in the colon during colitis.[43] In this condition, neutrophil infiltration into the damaged mucosa and increased neutrophil extracellular traps sustain inflammation by enhancing the release of TNF and IL-1β.[43] Circulating T cells migrate into the intestinal lamina propria. There, mediated by various cytokines, they differentiate into effector T cells or tissue-resident memory T cells, which exert pro- or anti-inflammatory effects.[44] While ulcerative colitis is often considered a Th2-skewed response,[44] the functional balance between Th17 and Treg cells is critically important. Studies indicate increased Th17 cells in the mucosa of colitis patients and elevated IL-17 in their blood.[45] In contrast, Treg cells suppress other T cells. Mouse models of colitis show decreased peripheral Treg cells, and their deficiency leads to more severe inflammation.[46] Evidence suggests that acetylcholine binding to α7nAChR-positive immune cells in the colon can reduce local pro-inflammatory cytokine release, thereby alleviating colitis.[12] This study provides the first experimental evidence that α7nAChR-positive immune cells may serve as a critical cellular mediator for the therapeutic effect of electro-acupuncture at ST37 on colonic inflammation. Our data suggest that the activation of the vagal cholinergic pathway by electroacupuncture likely culminates at these α7nAChR-expressing cells within the colon. The engagement of this

receptor is pivotal for translating the neural signal into a localized anti-inflammatory response. Therefore, these findings identify α7nAChR-positive immune cells as a key functional target in the neuro-immune axis activated by somatic electroacupuncture stimulation. This delineates a more precise mechanism through which peripheral acupuncture intervention alleviates systemic visceral inflammation.

While this study provides novel insights into acupuncture's therapeutic effects against colitis, several important limitations must be acknowledged. First, we cannot exclude the potential contribution of the vagal-adrenal anti-inflammatory pathway, which is also known to be activated by somatic acupuncture stimulation. Second, the precise identities of the local colonic immune cells that are the initial and direct targets of the acupuncture-initiated signal remain unclear. Determining whether they are macrophages, dendritic cells, or other α7nAChR-positive populations is a crucial next step. Finally, our investigation was specifically focused on the supraspinal vagal cholinergic pathway. We did not explore the potential role of the sacral parasympathetic nervous system, which is another key autonomic pathway governing pelvic organ function and inflammation. These limitations highlight specific avenues for future research to obtain a more complete mechanistic understanding.

In conclusion, this study demonstrates that electroacupuncture at ST37 alleviates colitis by activating ChAT-positive neurons in the DMV and stimulating the vagus nerve. This leads to the modulation of colonic α7nAChR-positive cells and engages the vagal cholinergic anti-inflammatory pathway. It provides the first experimental evidence that electro-acupuncture relieves visceral inflammation through this specific vagal nerve-mediated immune regulation. These findings advance the translational potential of acupuncture for colitis. Future research will focus on the roles of the sympathetic and sacro-parasympathetic systems.

Data Sharing Statement

The data that support the findings of this study are available from the corresponding author, Yangshuai Su, upon reasonable request.

Ethical Statement

This study protocol has been approved by the Ethics Committee of the Institute of Acupuncture and Moxibustion, China Academy of Chinese Medical Sciences on March 12, 2025, before experiments, with approval number Y2025-3-12-19. All experiments were conducted at the Institute of Acupuncture and Moxibustion, Chinese Academy of Chinese Medical Sciences.

Author Contributions

Zhengyang Qu contributed to this work through Formal analysis, Funding acquisition, Methodology, and Writing–original draft. Min Luo and Xiaoyu Liu contributed through Investigation and Validation, and Writing–original draft. Yangshuai Su contributed through Conceptualization, Funding acquisition, and Writing–review and editing. Xianghong Jing contributed through Conceptualization, Resources, Supervision, and Writing–review and editing. All authors gave final approval of the version to be published; have agreed on the journal to which the article has been submitted; and agree to be accountable for all aspects of the work.

Funding

This study is funded by National Natural Science Foundation of China (No. 82105033), the Special Training Program for Outstanding Young Scientific and Technological Talents (Innovation Category) of the China Academy of Chinese Medical Sciences (No. ZZ15-YQ-047, No. ZZ13-YQ-069), and the Independent Topic Selection for Basic Scientific Research Funds of the Institute of Acupuncture and Moxibustion, Chinese Academy of Chinese Medicine Sciences (No. ZZCZ2025-019). The funder only provides financial support and does not participate in research design, analysis, or reporting.

Disclosure

The authors declare that they have no known competing financial interests or personal relationships that could have appeared to influence the work reported in this paper.

References

1. da Luz Moreira A, de Campos Lobato L, de Souza H. 362 – IBD epidemiology: what is going on in the developing world? Results from 163,000 patients. Gastroenterology. 2019;156(6):S–73.
2. Høivik ML, Moum B, Solberg IC, Henriksen M, Cvancarova M, Bernklev T. Work disability in inflammatory bowel disease patients 10 years after disease onset: results from the IBSEN study. *Gut*. 2013;62:368–375. doi:10.1136/gutjnl-2012-302311
3. Cosnes J, Gower-Rousseau C, Seksik P, Cortot A. Epidemiology and natural history of inflammatory bowel diseases. *Gastroenterology*. 2011;140:1785–1794. doi:10.1053/j.gastro.2011.01.055
4. Liu S, Wang Z, Su Y, et al. A neuroanatomical basis for electroacupuncture to drive the vagal-adrenal axis. *Nature*. 2021;598(7882):641–645. doi:10.1038/s41586-021-04001-4
5. Yan-Qiu L, Jun-Peng Y, Xiang-Yun Y, et al. Advances in acupuncture regulation on the autonomic nervous system from 2013 to 2022: a bibliometric analysis via citespace. *Complement Ther Med*. 2024;80:103009. doi:10.1016/j.ctim.2023.103009
6. Goverse G, Stakenborg M, Matteoli G. The intestinal cholinergic anti-inflammatory pathway. *J Physiol*. 2016;594(20):5771–5780. doi:10.1113/JP271537
7. Ungaro R, Mehandru S, Allen PB, Peyrin-Biroulet L, Colombel JF. Ulcerative colitis. *Lancet*. 2017;389(10080):1756–1770. doi:10.1016/S0140-6736(16)32126-2
8. Ford AC, Kane SV, Khan KJ, et al. Efficacy of 5-aminosalicylates in Crohn's disease: systematic review and meta-analysis. *Am J Gastroenterol*. 2011;106:617–629. doi:10.1038/ajg.2011.71
9. Genovese MC, Gaylis NB, Sikes D, et al. Safety and efficacy of neurostimulation with a miniaturised vagus nerve stimulation device in patients with multidrug-refractory rheumatoid arthritis: a two-stage multicentre, randomised pilot study. *Lancet Rheumatol*. 2020;2:E527–E538. doi:10.1016/S2665-9913(20)30172-7
10. Jackson RG. Anatomy of the vagus nerves in the region of the lower esophagus and the stomach. *Anat Rec*. 1949;103(1):1–18. doi:10.1002/ar.1091030102
11. Qian BF, el-Salhy M, Danielsson A, Shalaby A, Axelsson H. Changes in intestinal endocrine cells in the mouse after unilateral cervical vagotomy. *Histol Histopathol*. 1999;14(2):453–460. doi:10.14670/HH-14.453
12. Stakenborg N, Labeeuw E, Gomez-Pinilla PJ, et al. Preoperative administration of the 5-HT4 receptor agonist prucalopride reduces intestinal inflammation and shortens postoperative ileus via cholinergic enteric neurons. *Gut*. 2019;68(8):1406–1416. doi:10.1136/gutjnl-2018-317263
13. Tsuchida Y, Hatao F, Fujisawa M, et al. Neuronal stimulation with 5-hydroxytryptamine 4 receptor induces anti-inflammatory actions via α7nACh receptors on muscularis macrophages associated with postoperative ileus. *Gut*. 2011;60(5):638–647. doi:10.1136/gut.2010.227546
14. Famm K, Litt B, Tracey KJ, Boyden ES, Slaoui M. Drug discovery: a jump-start for electroceuticals. *Nature*. 2013;496(7444):159–161. doi:10.1038/496159a
15. Magisetty R, Park SM. New era of electroceuticals: clinically driven smart implantable electronic devices moving towards precision therapy. *Micromachines*. 2022;13(2):161. doi:10.3390/mi13020161
16. Oke SL, Tracey KJ. The inflammatory reflex and the role of complementary and alternative medical therapies. *Ann NY Acad Sci*. 2009;1172. doi:10.1196/annals.1393.013
17. Sun P, Zhou K, Wang S, et al. Involvement of MAPK/NF-κB signaling in the activation of the cholinergic anti-inflammatory pathway in experimental colitis by chronic vagus nerve stimulation. *PLoS One*. 2013;8(8):e69424. doi:10.1371/journal.pone.0069424
18. Jin H, Guo J, Liu J, et al. Anti-inflammatory effects and mechanisms of vagal nerve stimulation combined with electroacupuncture in a rodent model of TNBS-induced colitis. *Am J Physiol Gastrointest Liver Physiol*. 2017;313(3):G192–G202. doi:10.1152/ajpgi.00254.2016
19. Sahn B, Pascuma K, Kohn N, Tracey KJ, Markowitz JF. Transcutaneous auricular vagus nerve stimulation attenuates inflammatory bowel disease in children: a proof-of-concept clinical trial. *Bioelectron Med*. 2023;9(1):23. doi:10.1186/s42234-023-00124-3
20. D'Haens G, Eberhardson M, Cabrijan Z, et al. Neuroimmune modulation through vagus nerve stimulation reduces inflammatory activity in crohn's disease patients: a prospective open-label study. *J Crohns Colitis*. 2023;17(12):1897–1909. doi:10.1093/ecco-jcc/jjad151
21. Liu S, Wang ZF, Su YS, et al. Somatotopic organization and intensity dependence in driving distinct NPY-Expressing sympathetic pathways by electroacupuncture. *Neuron*. 2020;108(3):436–450.e7. doi:10.1016/j.neuron.2020.07.015
22. Ma Q. Somatotopic organization of autonomic reflexes by acupuncture. *Curr Opin Neurobiol*. 2022;76:102602. doi:10.1016/j.conb.2022.102602
23. Lim HD, Kim MH, Lee CY, Namgung U. Anti-Inflammatory effects of acupuncture stimulation via the vagus nerve. *PLoS One*. 2016;11(3):e0151882. doi:10.1371/journal.pone.0151882
24. Ulloa L. Electroacupuncture activates neurons to switch off inflammation. *Nature*. 2021;598(7882):573–574. doi:10.1038/d41586-021-02714-0
25. Zhang X, Kang Y, Li T. Mechanism study of acupuncture and acupuncture combined with medication in the treatment of ulcerative colitis. *Physiol Res*. 2025;74(3):359–372. doi:10.33549/physiolres.935545
26. Sun X-Y, Wan H-Y, Zhang Z-Y. Mechanisms of electroacupuncture at "Zusanli"(ST36) in delaying colon "inflammation-cancer transformation". *Zhen Ci Yan Jiu*. 2022;47(10):866–871. doi:10.13702/j.1000-0607.20220329
27. Liu Z, Jiao Y, Yu T, et al. A review on the immunomodulatory mechanism of acupuncture in the treatment of inflammatory bowel disease. *Evid Based Complement Alternat Med*. 2022;2022:8528938. doi:10.1155/2022/8528938
28. Yu QQ, Li T, Zhnag ZY, et al. Improvement in colonic inflammatory injury in rats via activating dorsal cholinergic neurons of vagus with electroacupuncture at sensitized acupoints. *Zhongguo Zhen Jiu*. 2021;41(1):45–51. doi:10.13703/j.0255-2930.20200914-k0003
29. Xu J, Peng WR, Zhang D, et al. Marine sponge-derived alkaloid ameliorates DSS-induced IBD via inhibiting IL-6 expression through modulating JAK2-STAT3-SOCS3 pathway. *Int Immunopharmacol*. 2024;129:111576. doi:10.1016/j.intimp.2024.111576
30. Wang YL, Su YS, He W, Jing XH. Electroacupuncture relieved visceral and referred hindpaw hypersensitivity in colitis rats by inhibiting tyrosine hydroxylase expression in the sixth lumbar dorsal root ganglia. *Neuropeptides*. 2019;77:101957. doi:10.1016/j.npep.2019.101957
31. Reardon C, Murray K, Lomax AE. Neuroimmune communication in health and disease. *Physiol Rev*. 2018;98(4):2287–2316. doi:10.1152/physrev.00035.2017
32. Huh JR, Veiga-Fernandes H. Neuroimmune circuits in inter-organ communication. *Nat Rev Immunol*. 2020;20(4):217–228. doi:10.1038/s41577-019-0247-z

33. Pavlov VA, Tracey KJ. Neural regulation of immunity: molecular mechanisms and clinical translation. *Nat Neurosci*. 2017;20(2):156–166. doi:10.1038/nn.4477
34. Motagally MA, Neshat S, Lomax AE. Inhibition of sympathetic N-type voltage-gated Ca2+ current underlies the reduction in norepinephrine release during colitis. *Am J Physiol Gastrointest Liver Physiol*. 2009;296(5):G1077–84. doi:10.1152/ajpgi.00006.2009
35. Tu L, Gharibani P, Yin J, Chen JDZ. Sacral nerve stimulation ameliorates colonic barrier functions in a rodent model of colitis. *Neurogastroenterol Motil*. 2020;32(10):e13916. doi:10.1111/nmo.13916
36. Pasricha TS, Zhang H, Zhang N, Chen JDZ. Sacral nerve stimulation prompts vagally-mediated amelioration of rodent colitis. *Physiol Rep*. 2020;8 (1):e14294. doi:10.14814/phy2.14294
37. Bai A, Lu N, Guo Y, Chen J, Liu Z. Modulation of inflammatory response via alpha2-adrenoceptor blockade in acute murine colitis. *Clin Exp Immunol*. 2009;156(2):353–362. doi:10.1111/j.1365-2249.2009.03894.x
38. Mccafferty DM, Wallace JL, Sharkey KA. Effects of chemical sympathectomy and sensory nerve ablation on experimental colitis in the rat [J]. *Am J Physiol*. 1997;272(2 Pt 1):G272–80. doi:10.1152/ajpgi.1997.272.2.G272
39. Jacobson K, Mchugh K, Collins SM. Experimental colitis alters myenteric nerve function at inflamed and noninflamed sites in the rat. *Gastroenterology*. 1995;109(3):718–722. doi:10.1016/0016-5085(95)90378-X
40. Straub RH, Grum F, Strauch U, et al. Anti-inflammatory role of sympathetic nerves in chronic intestinal inflammation. *Gut*. 2008;57(7):911–921. doi:10.1136/gut.2007.125401
41. Ağaç D, Estrada LD, Maples R, Hooper LV, Farrar JD. The β2-adrenergic receptor controls inflammation by driving rapid IL-10 secretion. *Brain Behav Immun*. 2018;74:176–185. doi:10.1016/j.bbi.2018.09.004
42. Borovikova LV, Ivanova S, Zhang M, et al. Vagus nerve stimulation attenuates the systemic inflammatory response to endotoxin. *Nature*. 2000;4056785:458–462.
43. Dinallo V, Marafini I, Di Fusco D, et al. Neutrophil extracellular traps sustain inflammatory signals in ulcerative colitis. *J CROHNS COLITIS*. 2019;13(6):772–784. doi:10.1093/ecco-jcc/jjy215
44. Zenewicz LA, Antov A, Flavell RA. CD4 T-cell differentiation and inflammatory bowel disease. *Trends Mol Med*. 2009;15(5):199–207. doi:10.1016/j.molmed.2009.03.002
45. Veldhoen M, Hocking RJ, Atkins CJ, Locksley RM, Stockinger B. TGFbeta in the context of an inflammatory cytokine milieu supports de novo differentiation of IL-17-producing T cells. *Immunity*. 2006;24(2):179–189. doi:10.1016/j.immuni.2006.01.001
46. Velikova TV, Miteva L, Stanilov N, et al. Interleukin-6 compared to the other Th17/Treg related cytokines in inflammatory bowel disease and colorectal cancer. *World J Gastroenterol*. 2020;26(16):1912–1925. doi:10.3748/wjg.v26.i16.1912

Journal of Inflammation Research

Dovepress
Taylor & Francis Group

Publish your work in this journal

The Journal of Inflammation Research is an international, peer-reviewed open-access journal that welcomes laboratory and clinical findings on the molecular basis, cell biology and pharmacology of inflammation including original research, reviews, symposium reports, hypothesis formation and commentaries on: acute/chronic inflammation; mediators of inflammation; cellular processes; molecular mechanisms; pharmacology and novel anti-inflammatory drugs; clinical conditions involving inflammation. The manuscript management system is completely online and includes a very quick and fair peer-review system. Visit http://www.dovepress.com/testimonials.php to read real quotes from published authors.

Submit your manuscript here: https://www.dovepress.com/journal-of-inflammation-research-journal